JOURNAL OF TISSUE ENGINEERING AND REGENERATIVE MEDICINE
J Tissue Eng Regen Med 2018; **12**: e513–e522.
Published online 23 May 2017 in Wiley Online Library (wileyonlinelibrary.com) **DOI:** 10.1002/term.2321

RESEARCH ARTICLE

Bioactive coating of decellularized vascular grafts with a temperature-sensitive VEGF-conjugated hydrogel accelerates autologous endothelialization *in vivo*

Makoto Iijima[1†], Hug Aubin[1†], Meike Steinbrink[1], Franziska Schiffer[1], Alexander Assmann[1], Richard D. Weisel[2], Yoshiro Matsui[3], Ren-Ke Li[2], Artur Lichtenberg[1*] and Payam Akhyari[1]
[1]*Department of Cardiovascular Surgery and Research Group for Experimental Surgery, Heinrich Heine University, Medical Faculty, Düsseldorf, Germany*
[2]*Toronto General Research Institute, University Health Network and Department of Surgery, Division of Cardiovascular Surgery, University of Toronto, Toronto, Ontario, Canada*
[3]*Department of Cardiovascular and Thoracic Surgery, Hokkaido University, Graduate school of Medicine, Sapporo, Japan*

Abstract

No ideal small-diameter vascular graft for widespread clinical application has yet been developed and current approaches still suffer from graft failure because of thrombosis or degeneration. Decellularized vascular grafts are a promising strategy as they preserve native vessel architecture while eliminating cell-based antigens and allow for autologous recellularization. In the present study, a functional *in vivo* rodent aortic transplantation model was used in order to evaluate the benefit of bioactive coating of decellularized vascular grafts with vascular endothelial growth factor (VEGF) conjugated to a temperature-sensitive aliphatic polyester hydrogel (HG). Luminal HG-VEGF coating persistence up to 4 weeks was confirmed *in vivo* by rhodamine-labelling. Doppler-sonography showed that the grafts were functional for up to 8 weeks *in vivo*. Histological and immunohistochemical analysis of the explanted grafts after 4 weeks and 8 weeks *in vivo* demonstrated significantly increased endothelium formation in the HG-VEGF group compared with the control group (luminal surface covered with single-layered endothelium, 4 weeks: 64.8 ± 7.6% vs. 40.4 ± 8.3%, $p = 0.025$) as well as enhanced media recellularization (absolute cell count, 8 weeks: 22.1 ± 13.0 vs. 3.2 ± 3.6, $p = 0.0039$). However, HG-VEGF coating also led to increased neo-intimal hyperplasia, resulting in a significantly increased intima-to-media ratio in the perianastomotic regions (intima-to-media ratio, 8 weeks: 1.61 ± 0.17 vs. 0.93 ± 0.09, $p = 0.008$; HG-VEGF vs. control). The findings indicate that HG-VEGF coating has potential for the development of engineered small-diameter artificial grafts, although further research is needed to prevent neo-intimal hyperplasia. **Copyright © 2016 John Wiley & Sons, Ltd.**

Received 23 March 2016; Revised 6 July 2016; Accepted 26 September 2016

Keywords **vascular endothelial growth factor; temperature-sensitive hydrogel; decellularized small-diameter aortic grafts; *de novo* endothelialization; vascular tissue engineering; biofunctionalization**

1. Introduction

With a 100 000 patients undergoing coronary and peripheral vessel bypass surgery every year, there is an urgent need to develop functional small-diameter artificial vascular grafts for clinical applications. Since the first report of a clinically successful artificial vascular implant in by Blakemore and Voorhees in 1954, a number of studies have determined the conditions for ideal artificial vascular implants: safety, non-immunogenicity as well as low risk of thrombogenicity, infection and degeneration in the acute and chronic post-transplant phase (L'Heureux *et al*., 1998; Kerdjoudj *et al*., 2007; Diao *et al*., 2010). However, despite a multitude of experimental and preclinical models, an ideal small-diameter artificial vascular implant for widespread clinical application has not yet been developed, as current approaches still deal with early and late graft failure caused by severe thrombogenesis and adverse immune response mechanisms, leading to degeneration (Isenberg *et al*., 2006).

In the past decade, advances in regenerative medicine, such as tissue engineering (Langer and Vacanti, 1993), have promoted novel approaches, leading to the engineering of bio-artificial vascular grafts. Here, one of the most promising strategies is the employment of decellularized tissues as scaffold material (Constantinescu *et al*., 2014; Sheridan *et al*., 2014a,b), as decellularization preserves the ultrastructural composition and microarchitecture of the native extracellular matrix (ECM), while eliminating cell-based antigens (Akhyari *et al*., 2011). However, as non-autologous ECM components and remnants of immunogenic donor material resulting from incomplete decellularization may still lie in direct contact with the blood stream after implantation, early functional autologous luminal endothelialization of the grafts is of

*Correspondence to: A. Lichtenberg, Department of Cardiovascular Surgery, Heinrich-Heine-University Düsseldorf, Moorenstrasse 5, 40225 Düsseldorf, Germany. E-mail: artur.lichtenberg@med.uni-duesseldorf.de
†Both authors contributed equally.

Copyright © 2016 John Wiley & Sons, Ltd.

crucial importance in order to prevent thrombotic events and graft degeneration (Tschoeke *et al*., 2009; Dahan *et al*., 2012; Padalino *et al*., 2012; Chu *et al*., 2013).

Recently, it was shown that bioactive coating of decellularized vascular grafts enhances autologous endothelialization and promotes functional neovessel remodelling (Cai *et al*., 2009; Assmann *et al*., 2013; Aubin *et al*., 2016; Koobatian *et al*., 2016). In the present study, a functional rodent aortic transplantation model (Assmann *et al*., 2012) was used in order to evaluate the functional performance of decellularized genuine small-diameter grafts (vessel diameter $\leq$ 2 mm) coated with a temperature-sensitive, aliphatic polyester hydrogel (HG) conjugated with vascular endothelial growth factor (VEGF) allowing sustained growth factor release (Wu *et al*., 2011), which has already successfully been used for infarct stabilization and cardiac repair in a small-animal myocardial infarction model (Wu *et al*., 2011).

As VEGF is known to play an important role in angiogenesis as well as in vasculogenesis, promoting endothelial cell (EC) migration and proliferation (Karamysheva, 2008), it has already been extensively studied in a multitude of *in vitro* and *in vivo* studies in the past, which demonstrated its striking potential to promote vascular growth, even when used as sole stimulating factor (Martino *et al*., 2015). As Koobatian *et al*. (2016) recently demonstrated the positive effects of functionalization of acellular native-ECM derived vascular grafts with VEGF in an ovine carotid artery interposition model, it was hypothesized that HG-VEFG coating might have great potential in enhancing endothelialization and guiding functional remodelling of genuine small-diameter tissue-engineered vascular grafts.

2. Materials and methods

All animal experiments were performed in accordance with the Guide for the Care and Use of laboratory Animals published by the US National Institutes of Health (National Research council, 2010. Guide for the care and use of laboratory animals. National Academies Press), and approved by the animal care committee of the Heinrich-Heine-University as well as local governmental authorities in NRW, Germany (reference number G/391/2012).

2.1. Functional rodent aortic transplantation model

A heterotopic aortic transplantation model was used for *in vivo* evaluation of functional performance of HG-VEGF coated grafts, as described previously (Assmann *et al*., 2012). Standard Wistar rats (male, 200–250 g) from an in-house breed of the local animal care facility were used for a rodent small-animal model. In total, 56 animals were used: 28 donor animals for graft harvesting and 28 recipient animals for graft implantation.

The recipient animals were randomly assigned to two experimental groups: HG-VEGF group (n = 10) received engineered aortic grafts coated with HG-VEGF, while the control group (n = 10) received uncoated grafts; each group was observed for 4 weeks (n = 5) and 8 weeks (n = 5) weeks, respectively. An additional eight animals were used for the evaluation of *in vivo* HG-VEGF persistence, receiving fluorescence labelled grafts that were explanted either after 2 weeks (n = 4) or 4 weeks (n = 4) *in vivo*.

2.2. Preparation of donor aorta and graft decellularization

Aortic grafts were harvested from donor rats, as previously described (Assmann *et al*., 2102). Briefly, the animals were euthanized by CO_2 insufflation. After thoracotomy, thoracic aorta was dissected from surrounding tissue and a U-shaped aortic graft was prepared using a microscope (Nikon, Düsseldorf, Germany). Directly after harvesting, aortic grafts were placed in 50 ml tubes (Sigma-Aldrich, Darmstadt, Germany) and decellularized by subjecting them to a standard detergent-based protocol, as described previously (Assmann *et al*., 2102). Briefly, the decellularization process consisted of dynamic tissue incubation in four repetitive 12-h cycles with 0.5% sodium dodecyl sulfate (SDS) and 0.5% deoxycholate (DCA), followed by 24-h rinse in distilled water containing 0.05% sodium azide and three repetitive 24-h washing cycles with phosphate buffered saline (PBS) containing 1% penicillin/streptomycin. Decellularization quality was controlled as previously described, only using fully decellularized grafts for the subsequent experiments (Aubin *et al*., 2013). All chemicals required were obtained from Sigma-Aldrich and Merck (Darmstadt, Germany).

2.3. HG-VEGF coating of decellularized aortic grafts

The HG-VEGF employed had already been extensively characterized in a previous study, where it was used as injectable hydrogel for infarct stabilization and cardiac repair in a rodent myocardial infarction model (Wu *et al*., 2011). The HG-VEGF was prepared by conjugating VEGF to aliphatic polyester HG [poly (δ-valerolactone)-block-poly (ethylene glycol)-block-poly (δ-valerolactone); PVL-b-PEG-b-PVL], as previously described by Wu *et al*. (2011). The HG-VEGF changes its physical properties depending on the temperature environment, turning from a gel-like state at 37°C to a soluble state at room temperature (22°C). For polymerization of the temperature-sensitive hydrogel after storage at –20°C, HG-VEGF was heated once to 50°C in a water bath for 10 min, turning HG-VEGF into a solid state and then it was cooled down at room temperature to turn it into a soluble state for the coating process.

For selective coating of the inner luminal graft surface, a 17 G catheter and a 18 G catheter (Vasofix Safety; B. Braun, Melsungen, Germany) were inserted into the proximal and distal site of the decellularized aortic graft, respectively, while clipping the cervical aortic branches with titanium haemostatic clips (Vitalitec Inc., Plymouth,

Copyright © 2016 John Wiley & Sons, Ltd.

DOI: 10.1002/term

MA, USA). The aortic graft was then filled with soluble HG-VEGF (0.3 ml) at room temperature and warmed quickly to 37°C after sealing both ends of the graft, so that the polymer solution would polymerize into a gel-like state again inside the graft lumen. After subsequent incubation at 37°C for 12 h, the lumen of the graft was rinsed with PBS at room temperature, to solubilize and wash out excess, non-bonded HG-VEGF in order to ensure patency of the lumen (Figure 1a,b), and was then implanted directly to the animal. Non-coated grafts, serving as a control group, were treated accordingly, but using PBS alone in all steps. For fluorescent HG-VEGF labelling, rhodamine 6G (Sigma-Aldrich) at a concentration of 0.2 mM was added to the soluble HG-VEGF or PBS alone, and grafts were coated as described above.

2.4. Implantation of engineered aortic grafts

Recipient rats received heterotopic implantation of the engineered aortic grafts (approx. Graft diameter: 2 mm ascending aorta, 1 mm descending aorta; approximate wall thickness: 100–200 μm), as previously described (Assmann *et al*., 2012). Briefly, rats were anaesthetized with 2.0–2.5% isoflurane, and the central jugular vein was exposed. After median laparotomy, infra-renal aorta was dissected from the inferior vena cava, sparing lumbar arteries as much as possible. Heparin (100 IU/kg) was systemically administered through the central jugular vein, the infra-renal aorta was clamped, and the proximal side of the U-shaped aortic graft was anastomosed in an end-to-side manner, using a 10–0 monofilament, non-absorbable polypropylene suture (Ethicon, Norderstedt, Germany). After temporal reperfusion through the lower limb to prevent paraplegia, the distal side of the graft was anastomosed in a similar fashion. Afterwards, sufficient patency of the graft was tested and the native aorta between the two anastomoses was ligated in order to maintain continuous blood flow through the implant (Figure 1c). Finally, the laparotomy was closed in a multilayered fashion and the recipient animals were allowed to recover from anaesthesia using carprofen 4.0 mg/kg subcutaneously as postoperative analgesic.

2.5. Sonographic evaluation of graft patency and cardiac function

For functional evaluation of the implanted grafts and cardiac function of recipient rats, transcutaneous echography was performed under 2.0% isoflurane anaesthesia immediately postoperatively and at 4 weeks and 8 weeks post-implantation using a Philips HDX11 ultrasonography system with a 15 MHz probe (Philips, Hamburg, Germany) (Figure 1d). Therefore, standard echocardiographic parameters were assessed, including the R–R interval (RR), left ventricular diastolic diameter (LVDd), left ventricular systolic diameter (LVDs), and ejection fraction (EF). The abdominal aorta was also examined from the renal arteries to the aortic bifurcation. Aortic graft diameter was measured at the proximal anastomosis (PA), midgraft (MG) and distal anastomosis site (DA). Peak systolic velocity (PSV) was measured to detect any functional stenosis. PSV-max was defined as the maximum PSV in the stenosis region, and the PSV ratio was calculated as PSV-max divided by PSV in the pre- or post-stenotic regions. A significant stenosis was defined as PSV-max of >250 cm/s (Idu *et al*., 2009).

2.6. Explantation of engineered aortic grafts

Rats were anesthetized as described above at 4 weeks or 8 weeks after implantation, respectively. After median laparotomy, the implanted aortic grafts were rinsed with heparin solution in PBS (12.5 IU/ml), excised, embedded in KP-Cryo-Compound® medium (Klinipath BV, Duiven, the Netherlands) and processed via cryostat sectioning (CM 1950; Leica, Wetzlar, Germany) using standard protocols.

2.7. Histological graft analysis

For histological analysis, frozen sections of 5 μm were stained with haematoxylin and eosin (H&E) and Movat's pentachrome staining according to standard protocols and then visualized using a transmission light microscope (DM 2000; Leica) equipped with a digital camera (DFC 425C; Leica) and the Leica Application Suite v3.7

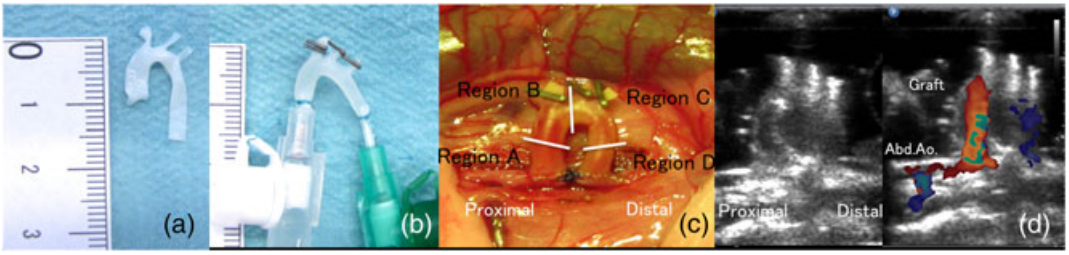

Figure 1. Selective luminal temperature-sensitive aliphatic polyester hydrogel–vascular endothelial growth factor (HG-VEGF) coating of decellularized aortic grafts and functional aortic transplantation model. After decellularization (a), two catheters were inserted into each end of the decellularized aortic graft and cervical branches were clipped using titanium haemostatic clips (b). Through the catheters, the decellularized aortic graft was filled with soluble HG-VEGF and subsequently polymerized to solid state by 37°C incubation. (c) Representative intraoperative image of an implanted engineered aortic graft after reperfusion. Explanted grafts were divided into four regions: proximal ascending aorta (region A), distal ascending aorta (region B), proximal descending aorta (region C) and distal descending aorta (region D). (d) Doppler sonographic evaluation of graft patency

Copyright © 2016 John Wiley & Sons, Ltd.

software (Leica). For the following histomorphological analyses built-in functions of Image J v1.46 software (National Institutes of Health, Bethesda, MD, USA) were used.

To analyse luminal recellularization, explanted grafts were divided into four regions: proximal ascending aorta (region A), distal ascending aorta (region B), proximal descending aorta (region C), and distal descending aorta (region D) (Figure 1c). Luminal endothelialization was quantified in representative H&E-stained cross-sections of each region, by measuring the length of luminal single-layered endothelium (excluding hyperplasic regions with multilayered endothelium) as well as the inner circumference of the graft to determine the proportion of functionally endothelialized luminal surface (percentage of luminal surface covered with single-layered endothelium), as previously described (Aubin *et al*., 2016). Intimal hyperplasia was quantified by measuring the area of luminal neo-intima (including single-layered as well as multilayered endothelium) as well as the area of the media in representative H&E-stained cross-sections and calculating the intima-to-media ratio of each region (quotient of neo-intimal area and medial area of the graft). Finally, the total number of cells invading the medial part of the decellularized implants was counted for each cross-section.

2.8. Immunohistochemical graft analysis

Cryo-embedding, sectioning and fixation were performed as described above. The 5 μm cryosections were treated at room temperature for 10 min with 0.25% Triton-X-100 and for 1 h with 5% bovine serum albumin (Sigma-Aldrich) with 0.1% Tween-20 (Merck, Darmstadt, Germany) in PBS. The sections were then incubated with primary antibodies against von Willebrand factor (vWF); DAKO, Hamburg, Germany), α-smooth muscle actin (αSMA; Sigma-Aldrich), CD3 (Sigma- Aldrich) and CD68 (Abcam, Cambridge, UK) for 1 h at 37°C, and then with secondary Alexa448-conjugated antibodies (Invitrogen, Carlsbad, CA, USA) for 45 min in a humid chamber in the dark at room temperature; all antibodies were diluted in 1% bovine serum albumin (BSA) and 0.1% Tween-20 in PBS. Sections were covered with 4′,6-diamidino-2-phenylindole (DAPI)-containing Vectashield mounting medium (Vector Labs, Peterborough, UK), and images were acquired using a DM2000 microscope equipped with a digital camera DFC 425C and the Leica Application Suite v3.7 software (Leica).

2.9. Statistical analysis

All statistical analyses were performed with Stat View J-5.0 software (SAS Institute, Cary, NC, USA). The data are presented as mean ± standard deviation (SD). An unpaired *t*-test was used to compare the means of the two groups, and two-way analysis of variance (ANOVA) analyses were used to compare the differences between the time-points. A *p*-value less than 0.05 was considered statistically significant.

3. Results

3.1. Operative outcome

A total of 20 rats were operated, with 10 rats receiving a HG-VEGF coated decellularized aortic graft and 10 rats receiving a non-coated decellularized aortic graft, serving as controls. In additionally, eight rats received a rhodamine-labelled coated or non-coated graft. Overall survival to scheduled explantation was 100% in all groups. Mean operative time was 105.3 ± 6.1 min and mean abdominal aortic cross clamp time was 50.2 ± 6.6 min. There were no procedure related differences between groups (Table 1).

All recipient rats showed normal clinical function with no clinical or Doppler-sonographic signs of lower body malperfusion up to the explantation time-point. Somatic growth and gain in bodyweight was adequate in all groups, with an increase of bodyweight after 4 weeks and 8 weeks post-implantation from 231.0 ± 18.1 g to 374.4 ± 31.1 g and 461.2 ± 36.2 g, respectively, in the HG-VEGF group, and from 225.4 ± 15.5 g to 365.2 ± 28.7 g and 452.2 ± 31.5 g, respectively, in the control group, indicating no significant difference.

3.2. Functional graft analysis via Doppler-sonography

Doppler sonography showed no morphological graft changes, other than an increasing graft diameter over time (Table 2) with graft patency demonstrated at all measured time-points and with no functional differences between groups. Peak systolic velocity of blood flow measured at the proximal and distal graft sites decreased over time for each individual graft. During follow-up, there were no functional differences at either anastomotic region between groups. At explantation all HG-VEGF-coated as well as non-coated explanted decellularized aortic grafts were patent, without macroscopic thrombus formation in either of the grafts, corroborating Doppler sonographic results.

Table 1. Operative outcome

	HG-VEGF group	Control group	
n	10	10	
Operative time (min)	104.4 ± 4.8	106.2 ± 7.0	n.s.
AXC time (min)			
Proximal side	28.7 ± 3.5	29.0 ± 3.1	n.s.
Distal side	22.2 ± 2.1	20.5 ± 4.4	n.s.
Operative mortality (%)	0	0	

HG-VEGF, temperature-sensitive aliphatic polyester hydrogel–vascular endothelial growth factor; TAXC, aorta cross clamp; n.s., not significant.

Copyright © 2016 John Wiley & Sons, Ltd.

DOI: 10.1002/term

Table 2. Follow-up echocardiographic data

	HG-VEGF group			Control group		
	Day 0	4 weeks	8 weeks	Day 0	4 weeks	8 weeks
Cardiac data						
RR (min)	0.182 ± 0.02	0.225 ± 0.03	0.230 ± 0.03	0.171 ± 0.03	0.212 ± 0.04	0.220 ± 0.03
LVDd (mm)	5.23 ± 0.29	6.39 ± 0.55	7.02 ± 0.82	5.12 ± 0.39	6.46 ± 0.42	7.11 ± 0.74
LVDs (mm)	2.59 ± 0.12	3.41 ± 0.30	3.72 ± 0.69	2.51 ± 0.31	3.46 ± 0.75	3.81 ± 0.77
EF (%)	86.3 ± 2.51	79.5 ± 3.01	75.8 ± 3.95	85.0 ± 4.21	81.3 ± 3.91	76.6 ± 4.45
Outer diameter of the implant						
At PA (mm)	2.51 ± 0.28	2.55 ± 0.35	2.70 ± 0.41	2.39 ± 0.25	2.44 ± 0.31	2.64 ± 0.37
At MG (mm)	2.05 ± 0.20	2.15 ± 0.28	2.23 ± 0.31	1.98 ± 0.35	2.11 ± 0.36	2.25 ± 0.42
At DA (mm)	1.81 ± 0.25	1.89 ± 0.29	2.02 ± 0.35	1.76 ± 0.22	1.85 ± 0.30	1.95 ± 0.33
PSV-max						
At PA (cm/s)	211.3 ± 20.4	168.2 ± 22.4	146.8 ± 18.3	239.1 ± 25.2	158.9 ± 22.6	132.2 ± 24.7
At DA (cm/s)	194.5 ± 18.3	154.8 ± 21.3	145.5 ± 22.7	221.2 ± 25.1	160.4 ± 19.6	155.0 ± 17.2

RR, R-R interval; LVDd, left ventricular diastolic diameter; LVDs, left ventricular systolic diameter; EF, ejection fraction; PA, proximal anastomosis; MG, midgraft; DA, distal anastomosis; PSV-max, maximum peak systolic velocity.

3.3. Cardiac function after graft implantation

Echocardiographic parameters of recipient rats are summarized in Table 2. Although after implantation, RR, LVDd and LVDs tended to increase slightly, whereas EF tended to decrease, no signs of cardiac failure owing to increased afterload could be detected in either of the groups.

3.4. HG-VEGF coating efficacy and *in vivo* persistence

The efficacy of HG-VEGF coating and *in vivo* persistence were examined by fluorescence labelling of HG-VEGF. Rhodamine-labelled HG-VEGF-coated grafts showed an intense fluorescent signal throughout all graft layers, with complete matrix penetration and no evidence for non-coated luminal regions, which could still be detected after 2 and 4 weeks *in vivo*, but at decreased intensities (Figure 2a–c). In contrast, decellularized aortic grafts incubated solely with PBS and rhodamine, showed only a very faint fluorescence signal directly after the 12 h incubation period (Figure 2d). These findings indicate successful HG-VEGF integration and up to 4 weeks persistence on the decellularized aortic grafts.

3.5. Endothelium formation

After 4 weeks, explanted aortic grafts showed a high degree of luminal recellularization, with the neo-intima mainly presenting as a single-cell layer, although in some regions neo-intimal hyperplasia was visible (Figure 3). Immunohistochemical analysis revealed single-layer cells that stained vWF positive, identifying them as newly formed endothelium, while multilayered hyperplasic regions also stained positive for αSMA.

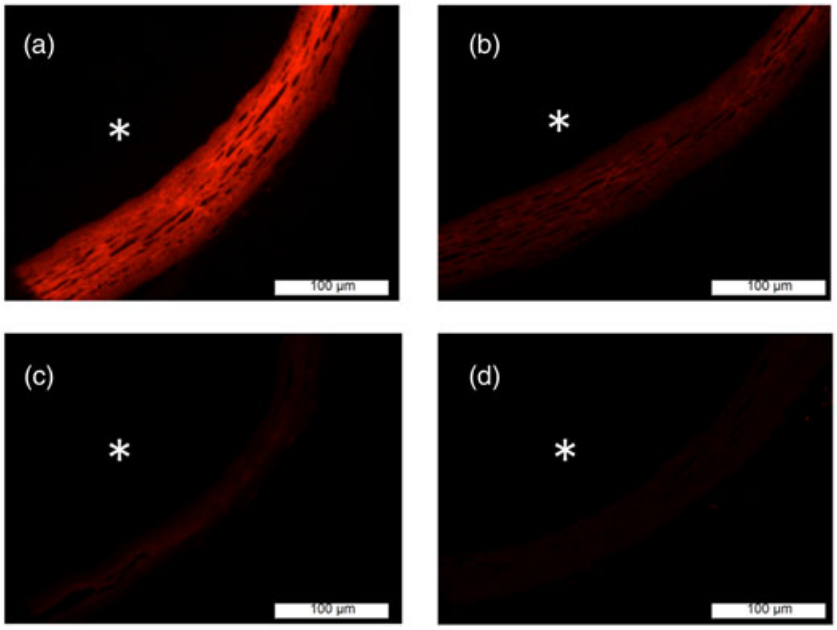

Figure 2. Coating efficacy and *in vivo* persistence of temperature-sensitive aliphatic polyester hydrogel–vascular endothelial growth factor (HG-VEGF). Decellularized aortic grafts coated with rhodamine-labelled HG-VEGF showed a strong fluorescence signal in the luminal graft layers directly after implantation (a). After 2 weeks (b) and 4 weeks (c), fluorescence could still be observed but at decreasing intensities. Control grafts coated solely with rhodamine plus phosphate-buffered saline showed only a very faint fluorescence signal immediately after incubation (d). *, Vessel lumen. Bar: 100 µm

Copyright © 2016 John Wiley & Sons, Ltd.

DOI: 10.1002/term

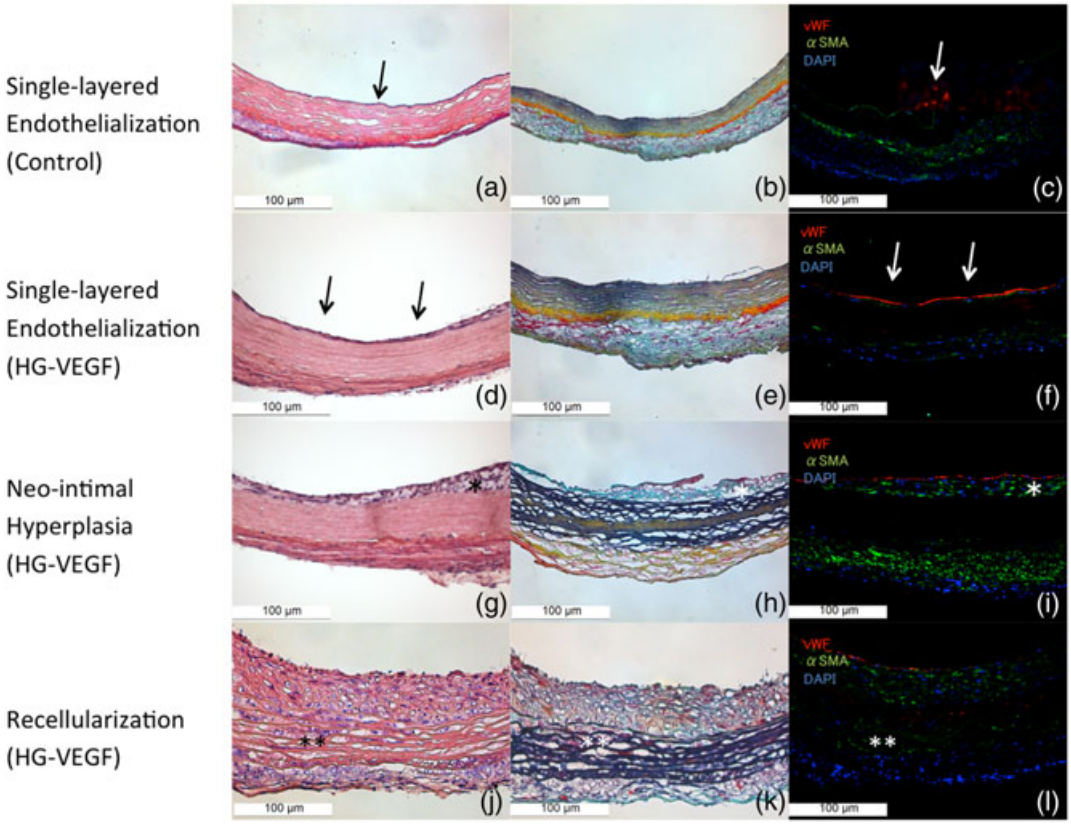

Figure 3. Luminal graft recellularization and recellularization of the media after 4 weeks *in vivo*. Representative images of haematoxylin and eosin (H&E) (a,d,g,j), Movat's pentachrome (b,e,h,k), and immunohistochemically (c,f,i,l) stained explanted temperature-sensitive aliphatic polyester hydrogel–vascular endothelial growth factor (HG-VEGF) coated and non-coated (control) aortic grafts (proximal ascending aortic region) after 4 weeks *in vivo*. Single-cell layer (arrows in a and d) on the luminal surface stained positive for von Willebrand factor (vWF; arrows in c and f), while multilayered hyperplastic regions (single asterisk in g) stained positive for α-smooth muscle actin (αSMA; single asterisk in i). Media-repopulating cells are marked with double asterisks in j–l. Red, vWF; green, αSMA; blue, 4′,6-diamidino-2-phenylindole (DAPI)

Functional endothelium formation was significantly increased in the HG-VEGF group compared with the control group (luminal surface covered with single-layered endothelium at 4 weeks, overall: 64.8 ± 7.6% vs. 40.4 ± 8.3%, $p = 0.025$) (Figure 4). Functional, single-layered endothelialization was especially present in the perianastomotic regions (luminal surface covered with single-layered endothelium, region A: 81.7 ± 6.9% vs. 52.9 ± 9.1%, $p = 0.021$; region D: 78.6 ± 7.1% vs. 54.8 ± 7.9%, $p = 0.019$; HG-VEGF vs. control, respectively), while the largest difference between the HG-VEGF-coated and the control group could be found in the proximal descending aortic part of the graft (luminal surface covered with single-layered endothelium, region C: 43.2 ± 8.1% vs. 31.2 ± 7.6%, $p = 0.215$).

After 8 weeks *in vivo*, endothelium formation further progressed with nearly the complete luminal surface of the grafts now being covered with vWF-positive cells. Differences in terms of functional, single-layered

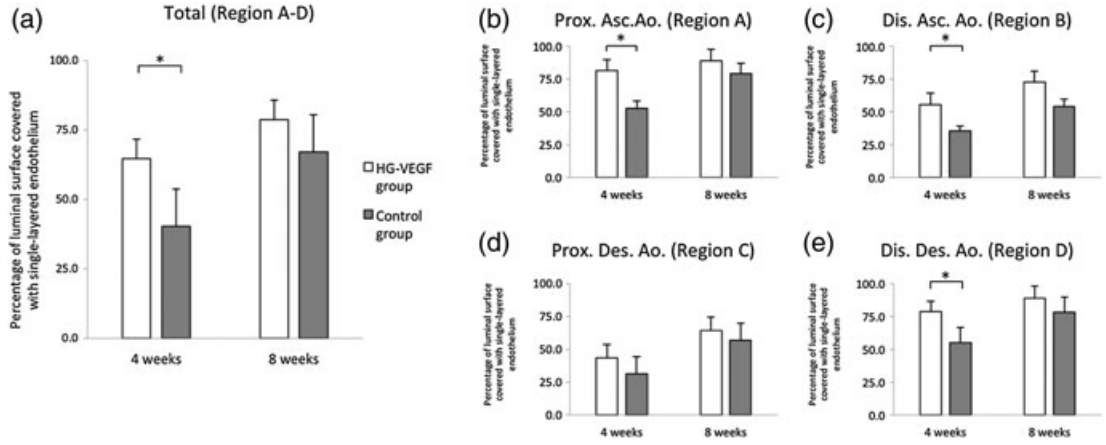

Figure 4. Functional endothelialization of decellularized aortic grafts after 4 weeks and 8 weeks *in vivo*. Percentage of luminal surface covered with single-layered endothelium in the corresponding regions of temperature-sensitive aliphatic polyester hydrogel–vascular endothelial growth factor (HG-VEGF)-coated and non-coated control grafts after 4 weeks and 8 weeks *in vivo*. Mean ± SD, $^*p < 0.05$

Copyright © 2016 John Wiley & Sons, Ltd.

DOI: 10.1002/term

endothelium between the HG-VEGF and the control group decreased, especially in the perianastomotic regions, although there was still a trend toward increased functional endothelium in the non-anastomotic regions (luminal surface covered with single-layered endothelium, region B: 72.6 ± 9.2% vs. 54.1 ± 10.4%; region C: 64.2 ± 8.8% vs. 57.1 ± 7.9%) (Figure 4).

Although HG-VEGF-coated grafts showed an increased percentage of functional, single-layered endothelium, the rate of neo-intimal hyperplasia was also increased compared with the non-coated control grafts. In addition, HG-VEGF specimens showed a strong augmentation of neo-intimal hyperplasia between the week 4 and week 8 *in vivo*, leading to a significantly increased intima-to-media ratio in the perianastomotic regions (intima-to-media ratio: region A: 1.61 ± 0.17 vs. 0.93 ± 0.09, $p = 0.008$; region D: 1.45 ± 0.29 vs. 0.83 ± 0.08, $p = 0.021$; HG-VEGF vs. control, 8 weeks, respectively) (Figure 5). In the non-anastomotic regions, the intima-to-media ratio was also increased for HG-VEFG-coated grafts compared with the non-coated grafts after 4 weeks as well as after 8 weeks *in vivo*, although there was no statistical significance.

3.6. Recellularization of the media

In addition to the newly formed endothelium, recellularization of the media of the implanted grafts was observed after 4 weeks and 8 weeks *in vivo* (Figure 3). Similar to the hyperplastic regions of the intima, a large number of αSMA-positive cells was also found in the media.

Media recellularization, in terms of absolute number of cells, was highly increased in the HG-VEGF group compared with the control group, both after 4 weeks and 8 weeks (7.3 ± 5.9 cells vs. 0.80 ± 1.2 cells, $p = 0.032$ after 4 weeks; 22.1 ± 13.0 cells vs. 3.2 ± 3.6 cells, $p = 0.0039$ after 8 weeks) (Figure 6). Just as for endothelium formation, the largest difference between groups was observed at the perianastomotic regions, reaching significance after 4 weeks. In the same regions, media recellularization in the HE-VEGF-coated grafts proceeded to increase considerably as time progressed, for example reaching a value eight times the absolute amount of media cells found in the non-coated grafts in the ascending aortic region of the graft after 8 weeks *in vivo*.

3.7. Inflammatory/immune response

The presence of immune cells within recellularized explanted grafts, indicating an on-going inflammatory and/or immune response of the host organism to graft implantation, was assessed by immunohistochemical staining and revealed complete absence of T-cells ($CD3^+$ cells) or cells of macrophage lineage ($CD68^+$ cells) within the majority of coated and non-coated grafts after either 4 weeks or 8 weeks *in vivo* (Figure 7a–b,d–e). Although, in some of the explanted grafts the presence of single $CD68^+$ cells in the media (Figure 7c) or clustering of $CD68^+$ cells in adventitial graft regions (Figure 7e) could be observed sporadically. However, there was no evidence for immune cells in the graft intimal regions; neither was there an evident difference between groups. Furthermore, the sporadic presence of immune cells could not be correlated with clinical signs of infection within the host animals, or with functional graft impairment via Doppler sonographic analysis.

4. Discussion

The present study shows that coating of decellularized grafts with a temperature-sensitive, aliphatic polyester hydrogel (HG) conjugated with vascular endothelial growth factor (VEGF) (Wu *et al*., 2011) significantly enhanced autologous endothelialization and influenced neovessel remodelling in a functional *in vivo* rodent aortic transplantation model (Assmann *et al*., 2012).

Haemocompatibility of artificial tissues for regenerative medicine applications is highly important, as non-

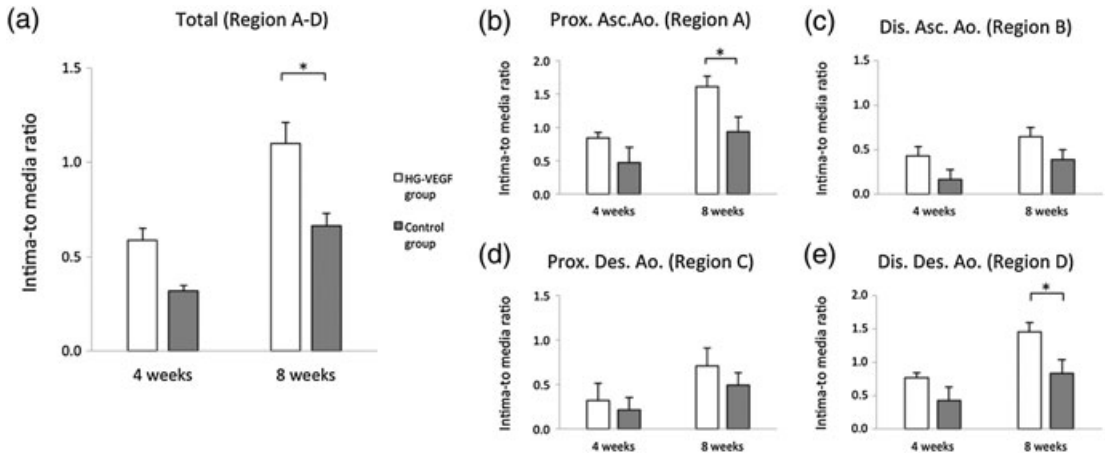

Figure 5. Neo-intimal hyperplasia of decellularized aortic grafts after 4 weeks and 8 weeks *in vivo*. Intima-to-media ratio in the corresponding regions of temperature-sensitive aliphatic polyester hydrogel–vascular endothelial growth factor (HG-VEGF)-coated and non-coated control grafts after 4 weeks and 8 weeks *in vivo*. Mean ± SD, *$p < 0.05$

Copyright © 2016 John Wiley & Sons, Ltd.

DOI: 10.1002/term

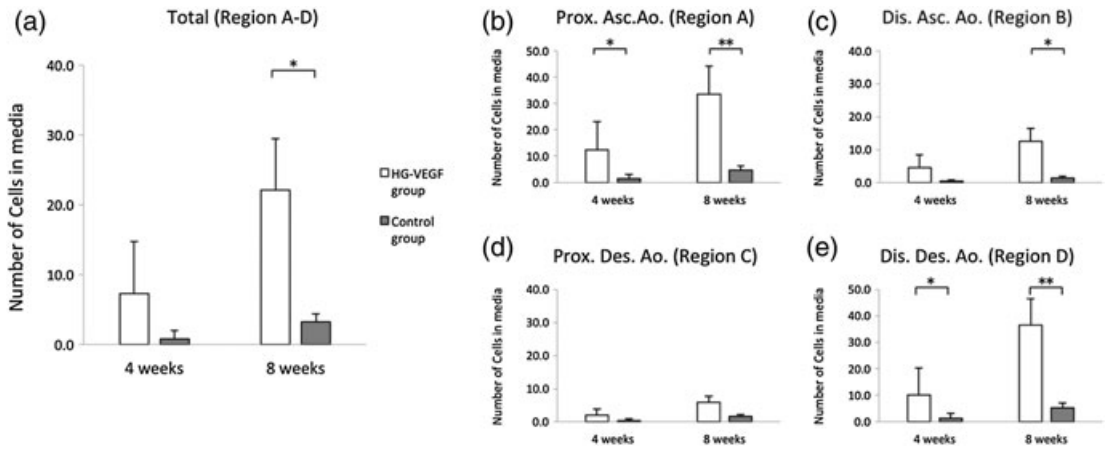

Figure 6. Recellularization of the media of decellularized aortic grafts after 4 weeks and 8 weeks *in vivo*. Absolute number of cells in the corresponding regions of temperature-sensitive aliphatic polyester hydrogel–vascular endothelial growth factor (HG-VEGF)-coated and non-coated control grafts after 4 weeks and 8 weeks *in vivo*. Mean ± SD, $^{*}p < 0.05$, $^{**}p < 0.01$

autologous and non-endothelialized surfaces lying in direct contact with the blood stream may trigger adverse biological effects, such as activation of platelet aggregation, leading to possible fatal thrombosis. In the case of small-diameter vascular grafts, where blood flow is limited by geometrical constraints, graft failure owing to thrombus formation and/or hyperplastic neo-intima with subsequent stenosis has been reported (Cai *et al*., 2009; Tschoeke *et al*., 2009). Therefore, functional endothelialization is of crucial importance for the *in vivo* performance of artificial small-diameter vascular implants.

Endothelialization of artificial surfaces may be achieved by *in vivo* cell recruitment through simple exposition to the blood stream or *ex vivo* cell- and bioreactor-based pre-implant procedures. The latter approach is complex as it requires time- and labour-intensive graft processing, with an increased risk of graft contamination. In addition, no optimal cell source for autologous *ex vivo* endothelialization has yet been found. Although endothelial progenitor cells (EPCs) have been proposed, among others, as a suitable cell source, the efficiency of EPC collection from peripheral blood is extremely low, and EPC purification and cultivation are challenging (Tan *et al*., 2013). Alternative cell sources, such as blood marrow mesenchymal stem cells and others, have similar issues regarding harvesting, cultivation and maturation to functional ECs (Joensuu *et al*., 2011).

It has been shown that exposition of decellularized ECM to the blood stream in physiologically functional *in vivo* models will lead to autologous surface endothelialization, which can further be enhanced by modification of the ECM–blood interface through bioactive coating (Cai *et al*., 2009; Assmann *et al*., 2013; Aubin *et al*., 2016; Koobatian *et al*., 2016). Here, VEGF embedded into a temperature-sensitive, aliphatic polyester hydrogel (PVL-b-PEG-b-PVL) was used to coat the luminal surface of decellularized aortic grafts. VEGF is a glycoprotein that binds to specific receptors on vascular ECs, which plays an important role in angiogenesis and vasculogenesis by promoting EC proliferation and maturation

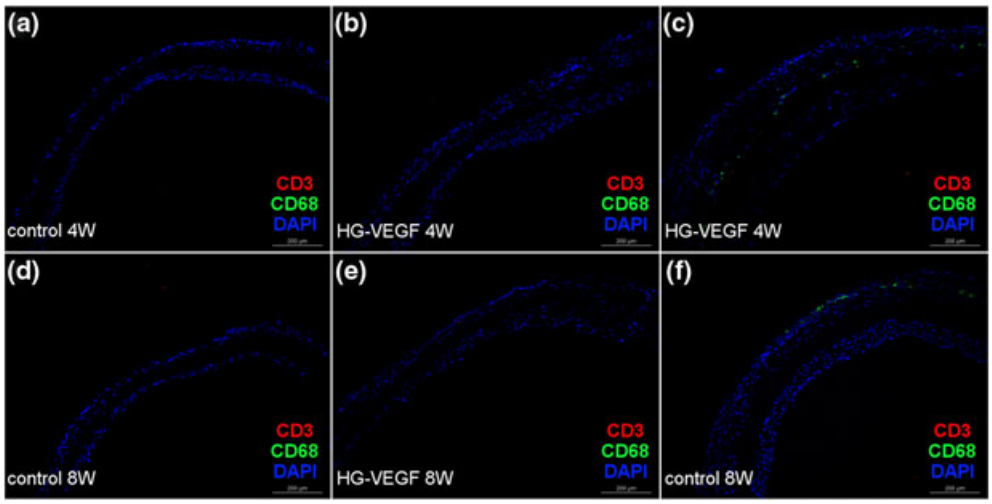

Figure 7. Presence of immune cells within decellularized aortic grafts after 4 weeks and 8 weeks *in vivo*. Representative images of CD3- and CD68-stained explanted temperature-sensitive aliphatic polyester hydrogel–vascular endothelial growth factor (HG-VEGF)-coated and non-coated (control) aortic grafts (proximal ascending aortic region) after 4 weeks and 8 weeks *in vivo* (a,b,d,e), showing complete absence of immune cells within recellularized grafts. Exemplary images of sporadic presence of single $CD68^{+}$ cells in the media (c) or clustering of $CD68^{+}$ cells in adventitial graft regions (e) of explanted HG-VEGF-coated and non-coated aortic grafts after 4 weeks and 8 weeks *in vivo,* respectively. Red, CD3; green, CD68; blue, 4′,6-diamidino-2-phenylindole (DAPI)

Copyright © 2016 John Wiley & Sons, Ltd.

DOI: 10.1002/term

(Karamysheva, 2008). Therefore, VEGF has the potential to stimulate EC adhesion to ligands of the basement membrane, to stabilize the neo-endothelium in front of sher forces generated by the blood stream and to promote functional neo-endothelium formation. By conjugating VEGF to a biodegradable hydrogel, a sustained effect is achieved, as it is gradually released while the biomaterial slowly degrades (Wu *et al*., 2011). In the present study, temperature-sensitive PVL-b-PEG-b-PVL was employed as a carrier substrate. This is a relatively inert synthetic HG, which is also used for targeted drug delivery systems (Zeng *et al*., 2006) and is characterized by a uniform honeycomb-like structure and pore size of approximately 1 μm, facilitating protein and peptide diffusion, as well as interaction between cells and ECM (Wu *et al*., 2011). Further, gelation at 37°C ensures retention of the HG coating at the luminal graft surface under systemic circulation, while the coating procedure can easily be performed with the HG in a liquid state at room temperature.

In the *in vivo* model system employed, HG-VEGF was shown to be persistent on the coated decellularized aortic grafts up to 4 weeks, despite exposure to plasmatic enzymes in the systemic blood circulation. In accord with the reported protein release kinetics and *in vivo* degradation profile, with full degradation of PVL-b-PEG-b-PVL within 6 weeks after subcutaneous implantation (Wu *et al*., 2011), fluorescently labelled HG-VEGF intensity decreased over time within the *in vivo* model employed. However, VEGF was present until neo-endothelium formation was almost concluded. The HG-VEGF coating significantly accelerated neo-endothelium formation with an increased percentage of luminal graft surface covered by single-layer endothelium at 4 weeks post-implantation. This effect was particularly obvious in the perianastomotic regions, which is consistent with the observation that luminal recellularization of vascular grafts may mainly be driven by cellular ingrowth from anastomotic regions (Assmann *et al*., 2013).

Finally, after 8 weeks *in vivo* the non-coated control group started to show a degree of endothelialization similar to that observed in the HG-VEGF group, however, at this point intimal hyperplasia was significantly increased in the HG-VEGF-coated grafts compared with the non-coated control group. Interestingly, increased neo-intimal hyperplasia after bioactive luminal surface coating of vascular grafts has been observed in the same rodent aortic transplantation model (Assmann *et al*., 2013; Aubin *et al*., 2016), but also in different preclinical animal models (Bastijanic *et al*., 2016) independent of the coating agent employed. Reasons for this still remain unclear, although in a clinical setting, such as polytetrafluoroethylene (PTFE) graft failure, neo-intimal hyperplasia is commonly triggered by foreign body reaction, which, however, could neither be observed in this nor in the previous studies (Assmann *et al*., 2013; Aubin *et al*., 2016). Further, as neo-intimal hyperplasia was significantly less in the non-coated grafts than in the coated grafts, the trigger may lie in the bioactive agent itself, rather than in the engineered graft or in an inflammatory and/or immune response of the host organism. It is worth noting, that VEGF not only regulates physiological angiogenesis but also pathological vascular growth (Martino *et al*., 2015), with, for example proper vascular morphogenesis depending on VEGF isoform balance and matrix-binding affinity (Ruhrberg *et al*., 2002). Therefore, VEGF and other bioactive agents might not only enhance endothelialization but also trigger a pathological response, leading to pathological neo-intima formation. Further research identifying causal pathways and finding strategies to prevent neo-intimal formation is therefore strongly warranted.

Although clinical assessment by Doppler-sonography showed no signs of relevant graft stenosis after 8 weeks, neo-intimal thickening might become a problem for long-term use as it may lead to graft stenosis, particularly in the most vulnerable perianastomotic regions, leading to late graft failure. Nonetheless, the strategy of using a temperature-sensitive HG as a carrier substrate for bioactive graft coating may easily allow the integration of one or more anti-proliferative agents into the existing platform. Here, further research is also warranted.

Interestingly, media repopulation was strongly enhanced in the HG-VEGF-coated grafts, showing such levels of cell infiltrations that, in contrast to the luminal endothelialization, could not be matched by the control group even after 8 weeks *in vivo*. This is consistent with the presence of fluorescently labelled HG-VEGF throughout all vascular graft layers, despite selective surface coating, and may be explained by the small molecular size of the HG-VEGF and the porosity of the decellularized aortic grafts (Brown *et al*. 2010), leading to HG diffusion throughout the entire ECM scaffold. Therefore, in addition to enhancing luminal endothelialization, HG-VEGF coating may also positively influence neovessel remodelling (Rustemever *et al*., 2007).

Although, in agreement with previous studies (Aubin *et al*., 2016), immunohistological analysis revealed complete absence of T-cells ($CD3^+$ cells) or cells of macrophage lineage ($CD68^+$ cells) within the majority of coated and non-coated grafts after either 4 weeks or 8 weeks *in vivo*, in some isolated cases, the presence of single $CD68^+$ cells in the media or clustering of mostly $CD68^+$ cells and single $CD3^+$ cells in adventitial graft regions could also be observed at irregular intervals. As the presence of macrophages within the neovessel might lead to positive remodelling (Ogle *et al*., 2016), and this process may inadequately be captured by punctual immunohistochemical staining, further studies assessing the possible impact of a low-profile immune response to graft remodelling are warranted.

4.1. Limitations

Although the present study has illustrated the effectiveness of HG-VEGF coating for accelerating autologous graft endothelialization in an *in vivo* model

Copyright © 2016 John Wiley & Sons, Ltd.

DOI: 10.1002/term

system, it has several limitations. First, degenerative processes such as microcalcification were not investigated, and these should be considered when evaluating the *in vivo* durability of decellularized tissue over longer observation periods (Dohmen *et al*., 2011; Della Barbera *et al*., 2014). Second, species-specific and age-dependent differences in EC proliferation activity should also be considered. Therefore, the results of animal experiments should be considered with caution when applied to humans. Further preclinical studies are warranted in order to translate these findings into a clinical setting.

5. Conclusion

The present study demonstrates that HG-VEGF coating of decellularized aortic grafts significantly accelerated autologous endothelialization and promoted medial recellularization in a physiologically functional *in vivo* model, possibly by sustained release of conjugated VEGF. The strategy employed has potential for the development of ideal small-diameter artificial vascular implants, although further research is needed, especially with regard to the prevention of neo-intimal hyperplasia.

Conflict of interest

The authors confirm that there are no known conflicts of interest associated with this publication and there has been no significant financial support for this work that could have influenced its outcome.

Acknowledgements

The authors gratefully acknowledge Susanne Bunnenberg-Stiftung (NRW, Germany) for her generous donation to the Research Group for Experimental Surgery of the Department of Cardiovascular Surgery of the Heinrich-Heine-University. The authors are also grateful to Gisela Müller for her assistance with histological staining.

References

Akhyari P, Aubin H, Gwanmesia P, *et al*. 2011; The quest for an optimized protocol for whole-heart decellularization of three popular and a novel decellularization technique and their diverse effects on crucial extracellular matrix qualities. *Tissue Eng Part C Methods* **17**: 915–926.

Assmann A, Akhyari P, Delfs C, *et al*. 2012; Development of a growing rat model for the *in vivo* assessment of engineered aortic conduits. *J Surg Res* **176**: 367–375.

Assmann A, Delfs C, Munakata H, *et al*. 2013; Acceleration of autologous *in vivo* recellularization of decellularized aortic conduits by fibronectin surface coating. *Biomaterials* **34**: 6015–6026.

Aubin H, Kranz A, Huelsmann J, *et al*. 2013; Decellularized whole heart for bioartificial heart. *Methods Mol Biol* **1036**: 163–178.

Aubin H, Mas-Moruno C, Iijima M, *et al*. 2016; Customized interface biofunctionalization of decellularized extracellular matrix: toward enhanced endothelialization. *Tissue Eng Part C Methods* **22**; 496–508.

Bastijanic, JM, Marchant RE, Kligman F, *et al*. 2016; *In vivo* evaluation of biomimetic fluorosurfactant polymer-coated expanded polytetrafluoroethylene vascular grafts in a porcine carotid artery bypass model. *J Vasc Surg* **63**; 1620–1630.

Blakemore AH, Voorhees AB Jr. 1954; The use of tubes constructed from vinyon N cloth in bridging arterial defects; experimental and clinical. *Ann Surg* **140**: 324–334.

Brown BN, Barnes CA, Kasick RT, *et al*. 2010; Surface characterization of extracellular matrix scaffolds. *Biomaterials* **31**: 428–437.

Cai WW, Gu YJ, Wang XN, *et al*. 2009; Heparin coating of small-caliber decellularized xenografts reduces macrophage infiltration and intimal hyperplasia. *Artif Organs* **33**: 448–455.

Chu Y, Lund DD, Weiss RM, *et al*. 2013; Pioglitazone attenuates valvular calcification induced by hypercholesterolemia. *Arterioscler Thromb Vasc Biol* **33**: 523–532.

Constantinescu A, Andrei E, Iordache F, *et al*. 2014; Recellularization potential assessment of Wharton's Jelly-derived endothelial progenitor cells using a human fetal vascular tissue model. *In Vitro Cell Dev Biol Anim* **50**: 937–944.

Dahan N, Zarbiv G, Sarig U, *et al*. 2012; Porcine small diameter arterial extracellular matrix supports endothelium formation and media remodeling forming a promising vascular engineered biograft. *Tissue Eng Part A* **18**: 411–422.

Della Barbera M, Valente M, Basso C, *et al*. 2014; Morphologic studies of cell endogenous repopulation in decellularized aortic and pulmonary homografts implanted in sheep. *Cardiovasc Pathol* **14**: 113–116.

Diao JS, Xia W, Guo SZ. 2010; Resume normal structure of epidermis and prevent hypertrophic scars formation. *Med Hypotheses* **74**: 85–86.

Dohmen PM, Lembcke A, Holinski S, *et al*. Ten years of clinical results with a tissue-engineered pulmonary valve. *Ann Thorac Surg* 2011; **92**: 1308–1314.

Idu MM, van Gulik TM, van Wijk B, *et al*. 2009; Glycerol-preserved arterial allografts evaluated in the infrarenal rat aorta. *Eur Surg Res* **42**: 78–86.

Isenberg BC, Williams C, Tranquillo RT. 2006; Small-diameter artificial arteries engineered *in vitro*. *Circ Res* **98**: 25–34.

Joensuu K, Paatero I, Alm JJ, *et al*. 2011; Interaction between marrow-derived human mesenchymal stem cells and peripheral blood mononuclear cells in endothelial cell differentiation. *Scand J Surg* **100**: 216–222.

Karamysheva AF. 2008; Mechanisms of angiogenesis. *Biochemistry (Mosc)* **73**: 751–762.

Kerdjoudj H, Moby V, Berthelemy N, Gentils M, Boura C, Bordenave L, Stoltz JF, Menu P. The ideal small arterial substitute: role of cell seeding and tissue engineering. *Clin Hemorheol Microcirc* 2007; **37**: 89–98.

Koobatian MT, Row S, Smith Jr, *et al*. 2016; Successful endothelialization and remodeling of a cell-free small-diameter arterial graft in a large animal model. *Biomaterials* **76**; 344–358.

L'Heureux N, Pâquet S, Labbé R, Germain L, Auger FA. 1998; A completely biological tissue-engineered human blood vessel. *FASEB J* **12**: 47–56.

Langer R, Vacanti JP. 1993; Tissue engineering. *Science* **260**: 920–926.

Martino MM, Brkic S, Bovo E, *et al*. 2015; Extracellular matrix and growth factor engineering for controlled angiogenesis in regenerative medicine. *Front Bioeng Biotechnol* **3**; 45–45.

National Research council. 2010; Guide for the care and use of laboratory animals. National Academies Press.

Ogle ME, Segar CE, Sridhar S, *et al*. 2016; Monocytes and macrophages in tissue repair: Implications for immunoregenerative biomaterial design. *Expl Bio Med* **241**; 1084–1097.

Padalino MA, Castellani C, Dedja A, *et al*. 2012; Extracellular matrix graft for vascular reconstructive surgery: evidence of autologous regeneration of the neoaorta in a murine model. *Eur J Cardiothorac Surg* **42**: 128–135.

Ruhrberg C, Gerhardt H, Golding M, *et al*. 2002; Spatially restricted patterning cues provided by heparin-binding VEGF-A control blood vessel branching morphogenesis. *Genes Dev* **16**: 2684–2698.

Rustemever P, Wittkowski W, Greve B, *et al*. 2007; Flow-cytometric identification, enumeration, purification, and expansion of $CD133^{+}$ and $VEGF\text{-}R2^{+}$ endothelial progenitor cells from peripheral blood. *J Immunoassay Immunochem* **28**: 13–23.

Sheridan WS, Grant OB, Duffy GP, *et al*. 2014a; The application of a thermoresponsive chitosan/β-GP gel to enhance cell repopulation of decellularized vascular scaffolds. *J Biomed Mater Res* **102**: 1700–1710.

Sheridan WS, Ryan AJ, Duffy GP, *et al*. 2014b; An experimental investigation of the effect of mechanical and biochemical stimuli on cell migration within a decellularized vascular construct. *Ann Biomed Eng* **42**: 2029–2038.

Sipehia R, Liszkowski M, Lu A. 2001; *In vivo* evaluation of ammonia plasma modified ePTFE grafts for small diameter blood vessels replacement. A preliminary report. *J Cardiovasc Surg (Torino)* **42**: 537–542.

Tan A, Goh D, Farhatnia Y, *et al*. 2013; An anti-CD34 antibody-functionalized clinical-grade POSS-PCU nanocomposite polymer for cardiovascular stent coating applications: a preliminary assessment of endothelial progenitor cell capture and hemocompatibility. *PLoS One* **8**: e77112.

Tschoeke B, Flanagan TC, Koch S, *et al*. 2009; Tissue-engineered small-caliber vascular graft based on a novel biodegradable composite fibrin-polylactide scaffold. *Tissue Eng Part A* **15**: 1909–1918.

Wu J, Zeng F, Huang XP, *et al*. 2011; Infarct stabilization and cardiac repair with a VEGF-conjugated, injectable hydrogel. *Biomaterials* **32**: 579–586.

Zeng F, Lee H, Allen C. 2006; Epidermal growth factor-conjugated poly (ethylene glycol)-block-poly (δ-valerolactone) copolymer micelles for targeted delivery of chemotherapeutics. *Bioconj Chem* **17**; 399–409.

Copyright © 2016 John Wiley & Sons, Ltd.